An alternative form of (26) may be obtained by using the following identity:

$$\sinh\left(\frac{\pi g}{2b}\right) = \frac{e^{(\pi g/2b)}}{\left[1 + \coth\left(\frac{\pi g}{2b}\right)\right]} \tag{28}$$

with the result

$$\frac{C_0}{\varepsilon_0 L} \simeq 4\left\{\frac{w}{b} + \frac{2}{\pi}\ln\left(1 + \coth\frac{\pi g}{2b}\right)\right\} - \frac{\Delta C}{\varepsilon_0 L}. \tag{29}$$

In this form it is easy to identify the first term in (29) as the plate capacitance between the stripline and the horizontal walls, and the second term as the fringing capacitance between the edges of the stripline and the side walls. For large gaps, the fringing term approaches $(8/\pi)$ ln 2, as expected [7, p. 515].

It is interesting to note that the first term on the right-hand side of (29) is the same formula given by Chen [7] and originally derived by Cohn [1]. Cohn's formula was derived assuming that the width of the center septum, $2w$, was very large compared to the plate separation, $2b$. This is equivalent to assuming that the two edges of the septum do not interact. ΔC, then, in (29) can be interpreted as a correction term needed to account for the interaction between the two edges. From (27) it can be seen that ΔC will be negligibly small if λ is near one (or λ' is near zero) since k is near one. From (15) λ'^2 is given approximately by

$$\lambda'^2 \simeq k'^2 \sinh^4\left(\frac{\pi g}{2b}\right). \tag{30}$$

It can be seen from (30) that for small gaps, λ' is always much less than one. For large gaps, it can be shown that (30) further reduces to

$$\lambda'^2 \simeq e^{-2\pi(w/b)} \tag{31}$$

by using the approximate expression for the modulus, k, given by Anderson [8]. From (31) it can easily be verified that λ' will be negligibly small, and hence ΔC may be neglected if

$$\frac{w}{b} \geq \frac{1}{2}. \tag{32}$$

In (21) we have the restriction that $\lambda^2 > 1/2$, or equivalently $\lambda'^2 < 1/2$. From (31) it can be seen that $\lambda'^2 < 1/2$ if

$$\frac{w}{b} \geq \frac{1}{2\pi}\ln 2 \simeq 0.1. \tag{33}$$

So for the range: $1/10 < w/b < 1/2$, ΔC is not negligible and must be calculated using (27), (31), and $k \simeq 1$.

The approximate formula for the capacitance given in (26) is plotted in Fig. 5 with a dashed line for $\Delta C = 0$. The exact formula using (6), (15), and (18) is plotted using a solid line. The two curves agree almost identically except where $w/b < 1/2$. This discrepancy can be attributed, however, to the ΔC term which was neglected.

Conclusions

The exact and an approximate form for the capacitance of the rectangular-coaxial-strip transmission line have been presented. The approximate form enables one to evaluate the edge-interaction capacitance for a limited range of w/b ratios. For w/b ratios greater than 1/2, our approximation was shown to reduce to those obtained by other authors who neglected the edge-interaction capacitance. Thus we have found the restrictions that must be observed when using their approximation.

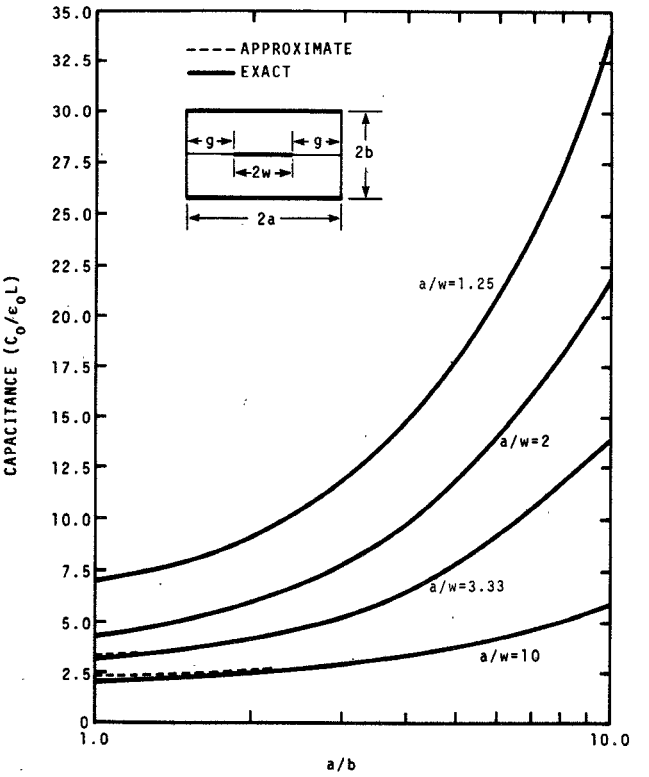

Fig. 5. Capacitance of a rectangular-coaxial-strip transmission line.

References

[1] S. B. Cohn, "Shielded coupled-transmission line," *IRE Trans. Microwave Theory Tech.*, vol. MTT-3, pp. 29–38, Oct. 1955.
[2] M. L. Crawford, "Generation of standard EM fields using TEM transmission cells," *IEEE Trans. Electromagnetic Compatibility*, vol. EMC-16, pp. 189–195, Nov. 1974.
[3] M. Walker, *The Schwarz-Christoffel Transformation and Its Applications—A Simple Exposition*. New York: Dover Publ. Inc., 1964.
[4] F. Bowman, *Introduction to Elliptic Functions With Applications*. New York: Dover Publ. Inc., 1961.
[5] M. Abramowitz and I. A. Stegun, *Handbook of Mathematical Functions*, 5th Ed. New York: Dover Publ. Inc., 1968, p. 612.
[6] E. T. Whittaker and G. N. Watson, *A Course of Modern Analysis*, 4th Ed. Cambridge: Cambridge University Press, 1969, p. 486.
[7] T.-S. Chen, "Determination of the capacitance, inductance, and characteristic impedance of rectangular lines," *IRE Trans. Microwave Theory Tech.*, vol. MTT-8, pp. 510–519, Sept. 1960.
[8] G. M. Anderson, "The calculation of the capacitance of coaxial cylinders of rectangular cross-section," *AIEE Trans.*, vol. 69, pt. II, pp. 728–731, 1950.

A Coplanar Waveguide with Thick Metal-Coating

T. KITAZAWA, Y. HAYASHI, AND M. SUZUKI, SENIOR MEMBER, IEEE

***Abstract*—A theoretical method is presented for the analysis of a coplanar waveguide with thick metal-coating. Numerical results are given and compared with published data. It is shown that the metal-coating thickness of the coplanar waveguide causes an increase in wavelength and a decrease in characteristic impedance and that the changes are about the same as those of a slot line.**

Introduction

A coplanar waveguide (CPW) has been investigated on the basis of a quasi-static approximation [1], [2], and recently Knorr and Kuchler [3] obtained the frequency dependence of

Manuscript received January 19, 1976; revised March 29, 1976.
The authors are with the Department of Electronic Engineering, Hokkaido University, Sapporo 060, Japan.

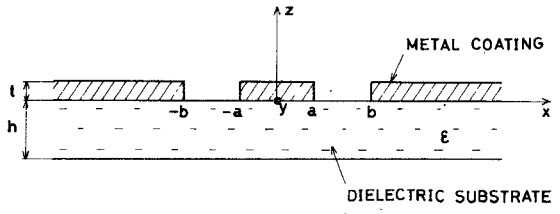

Fig. 1. Coplanar waveguide. ε is the dielectric constant.

the CPW by extending the method proposed by Itoh and Mittra [4]. These theories, however, neglect the effect of the metal-coating thickness. For the dispersion characteristics of a single slot line, the authors [5] employed the network analytical methods of electromagnetic fields [6] to evaluate the effect of the metal-coating thickness. In this short paper we extend this method to analyze the CPW with the metal-coating thickness greater than zero and evaluate the dispersion characteristics and characteristic impedance.

Determinantal Equation

A cross section of the CPW is shown in Fig. 1. First we express the transverse fields $\boldsymbol{E}_t$, $\boldsymbol{H}_t$ in the regions $z > t$, $t > z > 0$, $0 > z > -h$, and $-h > z$ by the following Fourier integral:

A. $z > t$, $0 > z > -h$, and $-h > z$; $-\infty < x < \infty$

$$\left.\begin{matrix}\boldsymbol{E}_t\\ \boldsymbol{H}_t\end{matrix}\right\} = \frac{1}{\sqrt{2\pi}} \sum_{l=1}^{2} \int_{-\infty}^{\infty} \exp(-j\beta y) \begin{Bmatrix} V_l(\alpha,\beta;z) f_l(\alpha,\beta;x) \\ I_l(\alpha,\beta;z) g_l(\alpha,\beta;x) \end{Bmatrix} d\alpha\, d\beta \tag{1}$$

where

$$f_1 = \frac{j}{\sqrt{2\pi}\,K}(x_0\alpha + y_0\beta)\exp(-j\alpha x)$$

$$f_2 = \frac{j}{\sqrt{2\pi}\,K}(x_0\beta - y_0\alpha)\exp(-j\alpha x)$$

$$g_l = z_0 \times f_l, \qquad (l = 1,2)$$

$$K = \sqrt{\alpha^2 + \beta^2}. \tag{2}$$

B. $t > z > 0$; $-b < x < -a$ (suffix L) and $a < x < b$ (suffix R)

$$\left.\begin{matrix}\boldsymbol{E}_{tR}\\ \boldsymbol{H}_{tR}\\ L\end{matrix}\right\} = \frac{1}{\sqrt{2\pi}} \sum_{l=1}^{2} \int_{-\infty}^{\infty} \sum_{n=0}^{\infty} \varepsilon_l(n) \cdot \exp(-j\beta y) \begin{Bmatrix} V_{lR}(\alpha_n,\beta;z) f_{lR}(\alpha_n,\beta;x) \\ I_{lR}(\alpha_n,\beta;z) g_{lR}(\alpha_n,\beta;x) \end{Bmatrix} d\beta \tag{3}$$

where

$$\varepsilon_l(n) = \begin{cases} 0, & (n = 0,\ l = 1) \\ 1/\sqrt{2}, & (n = 0,\ l = 2) \\ 1, & (n \neq 0) \end{cases}$$

$$f_{1R} = \frac{-1}{K_n}\sqrt{\frac{2}{W}}\left[x_0\alpha_n \cos\{\alpha_n(x \mp a)\} - y_0 j\beta \sin\{\alpha_n(x \mp a)\}\right]$$

$$f_{2R} = \frac{1}{K_n}\sqrt{\frac{2}{W}}\left[x_0 j\beta \cos\{\alpha_n(x \mp a)\} - y_0\alpha_n \sin\{\alpha_n(x \mp a)\}\right]$$

$$g_{lR} = z_0 \times f_{lR}, \qquad l = 1,2$$

$$\alpha_n = 2n\pi/W, \qquad K_n = \sqrt{\alpha_n^2 + \beta^2}, \qquad W = b - a. \tag{4}$$

C. $t > z > 0$; $|x| > b$ *and* $|x| < a$

$$\boldsymbol{E}_t = 0 \qquad \boldsymbol{H}_t = 0 \tag{5}$$

where x_0, y_0, and z_0 are unit vectors along the x, y, and z axes, respectively, and $l = 1$ and $l = 2$ represent E waves ($H_z = 0$) and H waves ($E_z = 0$), respectively. V_l and I_l are mode voltages and mode currents, and f_l and g_l are vector mode functions which satisfy boundary conditions

$$E_y = 0, \qquad \frac{\partial H_y}{\partial x} = 0$$

$$x = \pm a \text{ and } \pm b, \qquad 0 < z < t \tag{6}$$

and the following orthonormal properties:

$$\int_{-b}^{-a} g_{l'L}^*(\alpha_{n'},\beta;x) \cdot z_0 \times f_{lL}(\alpha_n,\beta;x)\, dx = \int_{a}^{b} g_{l'R}^*(\alpha_{n'},\beta;x) \cdot z_0 \times f_{lR}(\alpha_n,\beta;x)\, dx = \delta_{ll'}\,\delta_{nn'}$$

$$\int_{-\infty}^{\infty} g_{l'}^*(\alpha',\beta;x) \cdot z_0 \times f_l(\alpha,\beta;x)\, dx = \delta_{ll'}\,\delta(\alpha - \alpha') \tag{7}$$

$\delta_{ll'}$ Kronecker's delta;
$\delta(\alpha - \alpha')$ Dirac's δ-function;

where the asterisk signifies the complex conjugate function. The derivation of the determinantal equation for the propagation constant of CPW is a straightforward extension of that for a single slot line [5]. Denote by $\boldsymbol{m}_1(x')\exp(-j\beta_0 y)$ and $\boldsymbol{m}_2(x')\exp(-j\beta_0 y)$ the magnetic currents at $z = t$ and $z = 0$, respectively, where β_0 is a propagation constant. Considering the field continuity on the boundary surfaces, we obtain the determinantal equation for the propagation constant

$$-\int_{-b}^{b}\int_{-\infty}^{\infty}\left[\frac{\omega\varepsilon_0}{k_0}\bar{G}_1(\alpha,\beta_0;x \mid x') - \frac{k_0}{\omega\mu_0}\bar{G}_2(\alpha,\beta_0;x \mid x')\right]\cdot \boldsymbol{m}_1(x')\, d\alpha\, dx'$$

$$= \int_{a}^{b}\sum_{n=0}^{\infty}\left\{\frac{\omega\varepsilon_0}{\gamma_n}\bar{F}_{1R}(\alpha_n,\beta_0;x \mid x') - \frac{\gamma_n}{\omega\mu_0}\boldsymbol{F}_{2R}(\alpha_n,\beta_0;x \mid x')\right\}\cdot \tilde{\boldsymbol{m}}_1(\alpha_n,\beta_0;x')\, dx'$$

$$\int_{a}^{b}\sum_{n=0}^{\infty}\left\{\frac{\omega\varepsilon_0}{\gamma_n}\bar{F}_{1R}(\alpha_n,\beta_0;x \mid x') - \frac{\gamma_n}{\omega\mu_0}\bar{F}_{2R}(\alpha_n,\beta_0;x \mid x')\right\}\cdot \tilde{\boldsymbol{m}}_2(\alpha_n,\beta_0;x')\, dx'$$

$$= \int_{-b}^{b}\int_{-\infty}^{\infty}\left\{\frac{\omega\varepsilon_0}{k_0}\frac{1 + \frac{\varepsilon_r k_0}{k}\tan(kh)}{1 - \frac{k}{\varepsilon_r k_0}\tan(kh)}\bar{G}_1(\alpha,\beta_0;x \mid x') - \frac{k_0}{\omega\mu_0}\frac{1 - \frac{k}{k_0}\tan(kh)}{1 + \frac{k_0}{k}\tan(kh)}\bar{G}_2(\alpha,\beta_0;x \mid x')\right\}$$

$$\cdot\, \boldsymbol{m}_2(x')\, d\alpha\, dx' \tag{8}$$

where

$$k_0 = \sqrt{K'^2 - \omega^2\varepsilon_0\mu_0}, \qquad k = \sqrt{\omega^2\varepsilon\mu_0 - K'^2}$$

$$\gamma_n = \sqrt{K_n'^2 - \omega^2\varepsilon_0\mu_0}, \qquad \varepsilon_r = \varepsilon/\varepsilon_0$$

$$K' = \sqrt{\alpha^2 + \beta_0^2}, \qquad K_n' = \sqrt{\alpha_n^2 + \beta_0^2}$$

$$\tilde{m}_1 = \coth(\gamma_n t)m_1(x') - \operatorname{cosech}(\gamma_n t)m_2(x')$$

$$\tilde{m}_2 = \operatorname{cosech}(\gamma_n t)m_1(x') - \coth(\gamma_n t)m_2(x')$$

$$\bar{G}_l(\alpha,\beta_0; x \mid x') = g_l(\alpha,\beta_0;x)g_l^*(\alpha,\beta_0;x'), \qquad \text{Dyadic}$$

$$\bar{F}_{lR}(\alpha_n,\beta_0; x \mid x') = g_{lR}(\alpha_n,\beta_0;x)g_{lR}^*(\alpha_n,\beta_0;x'), \qquad l = 1,2$$

where x lies within the region $a < x < b$.

Characteristic Impedance

Because of the hybrid mode of propagation, the definition for characteristic impedance is not uniquely specified. The definition chosen here is

$$Z_0 = \frac{V_0^2}{2P_{\text{ave}}} \tag{9}$$

where V_0 is the peak voltage and P_{ave} is the average power flow along the y direction.

Numerical Procedure and Results

The determinantal equation (8) is exact, and involves x and y components of the vector magnetic current. If, however, the first-order approximation is used, the computation time can be reduced [3]. The width W is usually very small compared to a wavelength, so that for the lowest order hybrid mode the transverse magnetic current can be neglected. Ignoring the transverse magnetic current, the determinantal equation (8) results in the following integral representation:

$$\int_{-b}^{b}\int_{-\infty}^{\infty} \frac{1}{K'^2}\left\{\frac{\omega\varepsilon_0}{k_0}\alpha^2 - \frac{k_0}{\omega\mu_0}\beta_0^2\right\} m_{1y}(x') \cdot \exp[-j\alpha(x - x')]\, d\alpha\, dx'$$

$$= \frac{4\pi}{W}\int_a^b \sum_{n=0}^{\infty} \frac{1}{K_n'^2}\left\{\frac{\omega\varepsilon_0}{\gamma_n}\varepsilon_n'\alpha_n^2 - \frac{\gamma_n}{\omega\mu_0}\varepsilon_n''\beta_0^2\right\} \cdot \{\operatorname{cosech}(\gamma_n t)m_{2y}(x') - \coth(\gamma_n t)m_{1y}(x')\} \cdot \cos\{\gamma_n(x - a)\}\cos\{\gamma_n(x' - a)\}\, dx'$$

$$\frac{4\pi}{W}\int_a^b \sum_{n=0}^{\infty} \frac{1}{K_n'^2}\left\{\frac{\omega\varepsilon_0}{\gamma_n}\varepsilon_n'\alpha_n^2 - \frac{\gamma_n}{\omega\mu_0}\varepsilon_n''\beta_0^2\right\} \cdot \{\operatorname{cosech}(\gamma_n t)m_{1y}(x') - \coth(\gamma_n t)m_{2y}(x')\} \cdot \cos\{\gamma_n(x - a)\}\cos\{\gamma_n(x' - a)\}\, dx'$$

$$= \int_{-b}^{b}\int_{-\infty}^{\infty} \frac{1}{K'^2}\left\{\frac{\omega\varepsilon_0}{k_0}\frac{1 + \frac{\varepsilon_r k_0}{k}\tan(kh)}{1 - \frac{k}{\varepsilon_r k_0}\tan(kh)}\alpha^2 - \frac{k_0}{\omega\mu_0}\frac{1 - \frac{k}{k_0}\tan(kh)}{1 + \frac{k_0}{k}\tan(kh)}\beta_0^2\right\} \cdot m_{2y}(x')\exp[-j\alpha(x - x')]\, d\alpha\, dx' \tag{10}$$

where

$$\varepsilon_n' = \begin{cases} 0, & (n = 0) \\ 1, & (n \neq 0) \end{cases}$$

$$\varepsilon_n'' = \begin{cases} \frac{1}{2}, & (n = 0) \\ 1, & (n \neq 0) \end{cases}$$

where $m_{1y}(x')$ and $m_{2y}(x')$ are the longitudinal magnetic current on the surfaces $z = t$ and $z = 0$, respectively. The longitudinal magnetic-current distributions are unknown, so that appropriate trial functions must be selected. We assume the following distribution [3]:

$$m_{iy}(x') = \frac{m_{i0}}{\{1 - (2x - a - b)^2/(b - a)^2\}^{1/2}}, \qquad a < x < b, \quad i = 1,2 \tag{11}$$

where m_{10} and m_{20} are constant values. From (10) and (11) phase constant β_0 can be obtained by applying the numerical calculation method used in [5]. The resulting equation is given as follows:

$$\{G_1(\beta_0) - G_4(\beta_0)\} \cdot \{G_2(\beta_0) - G_4(\beta_0)\} = \{G_3(\beta_0)\}^2 \tag{12}$$

where

$$G_1(\beta_0) = \int_0^{\infty} \frac{1}{K'^2}\left\{\frac{\omega\varepsilon_0}{k_0}\alpha^2 - \frac{k_0}{\omega\mu_0}\beta_0^2\right\} J_0^2\left(\frac{b - a}{2}\alpha\right) \cdot \sin^2\left(\frac{a + b}{2}\alpha\right) d\alpha$$

$$G_2(\beta_0) = \int_0^{\infty} \frac{1}{K'^2}\left\{\frac{\omega\varepsilon_0}{k_0}\frac{1 + \frac{\varepsilon_r k_0}{k}\tan(kh)}{1 - \frac{k}{\varepsilon_r k_0}\tan(kh)}\alpha^2 - \frac{k_0}{\omega\mu_0}\frac{1 - \frac{k}{k_0}\tan(kh)}{1 + \frac{k_0}{k}\tan(kh)}\beta_0^2\right\} J_0^2\left(\frac{b - a}{2}\alpha\right) \cdot \sin^2\left(\frac{a + b}{2}\alpha\right) d\alpha$$

$$G_3(\beta_0) = \frac{\pi}{b - a}\left[\frac{\gamma_0}{2\omega\mu_0}\operatorname{cosech}(\gamma_0 t) - \sum_{n=1}^{\infty}\frac{1}{K_n'^2}\left\{\frac{\omega\varepsilon_0}{\gamma_n}\alpha_n^2 - \frac{\gamma_n}{\omega\mu_0}\beta_0^2\right\} \cdot \operatorname{cosech}(\gamma_n t)J_0^2\left(\frac{b - a}{2}\alpha_n\right) \cdot \cos^2\left(\frac{b - a}{2}\alpha_n\right)\right]$$

$$G_4(\beta_0) = \frac{\pi}{b - a}\left[\frac{\gamma_0}{2\omega\mu_0}\coth(\gamma_0 t) - \sum_{n=1}^{\infty}\frac{1}{K_n'^2}\left\{\frac{\omega\varepsilon_0}{\gamma_n}\alpha_n^2 - \frac{\gamma_n}{\omega\mu_0}\beta_0^2\right\} \cdot \coth(\gamma_n t)J_0^2\left(\frac{b - a}{2}\alpha_n\right)\cos^2\left(\frac{b - a}{2}\alpha_n\right)\right]$$

$J_0(x)$ zero-order Bessel function.

From (12) we can find the phase constant for the lowest hybrid mode, which is expected to be in the range $\beta_0 > \omega\sqrt{\varepsilon_0\mu_0}$. Substituting this value into (9), the characteristic impedance can be obtained. G_3 and G_4 converge very rapidly; however, the rate of convergence of G_1 and G_2 is slow and can be improved by the following procedure. When $\alpha \to \infty$, the integrand of G_1 becomes

$$K_{1\infty} = \lim_{\alpha\to\infty} K_1 = \frac{4}{\pi(b-a)}\left(\omega\varepsilon_0 - \frac{\beta_0^2}{\omega\mu_0}\right)\frac{1}{K'^2} \cdot \sin^2\left(\frac{a+b}{2}\alpha\right)\cos^2\left(\frac{b-a}{2}\alpha - \frac{\pi}{4}\right). \quad (13)$$

G_1 may be rewritten as follows:

$$G_1 = \int_0^\infty (K_1 - K_{1\infty})\,d\alpha + \int_0^\infty K_{1\infty}\,d\alpha. \quad (14)$$

The first integral on the right converges rapidly compared to G_1, while the second may be expressed in closed form as

$$\int_0^\infty K_{1\infty}\,d\alpha = \left(\omega\varepsilon_0 - \frac{\beta_0^2}{\omega\mu_0}\right)M(\beta_0)$$

where

$$\begin{aligned} M(\beta_0) = {} & \frac{1}{2\beta_0(b-a)}\left\{1 - \exp\left(-2\frac{b+a}{b-a}\beta_0\right)\right\} \\ & + \frac{1}{4\beta_0\pi(b-a)}\left[2\{\exp(-2\beta_0)\bar{E}_i(2\beta_0) \right. \\ & \left. - \exp(2\beta_0)E_i(-2\beta_0)\} \right. \\ & - \exp\left(-\frac{4b}{b-a}\beta_0\right)\bar{E}_i\left(\frac{4b}{b-a}\beta_0\right) \\ & + \exp\left(\frac{4b}{b-a}\beta_0\right)E_i\left(-\frac{4b}{b-a}\beta_0\right) \\ & + \exp\left(-\frac{4a}{b-a}\beta_0\right)\bar{E}_i\left(\frac{4a}{b-a}\beta_0\right) \\ & \left. - \exp\left(\frac{4a}{b-a}\beta_0\right)E_i\left(-\frac{4a}{b-a}\beta_0\right)\right] \end{aligned}$$

where $E_i(x)$, $\bar{E}_i(x)$ represent the exponential-integral function. Similarly, for G_2

$$G_2 = \int_0^\infty (K_2 - K_{2\infty})\,d\alpha + \left(\omega\varepsilon_0\varepsilon_r - \frac{\beta_0}{\omega\mu_0}\right)M(\beta_0).$$

In Fig. 2 the computed results, supposing the thickness equal to zero, are shown and compared with those from [3]. Note that the characteristic impedance of CPW, Z_0, given by (9) is one-half of the odd-mode characteristic impedance of coupled slots, Z_{oo},

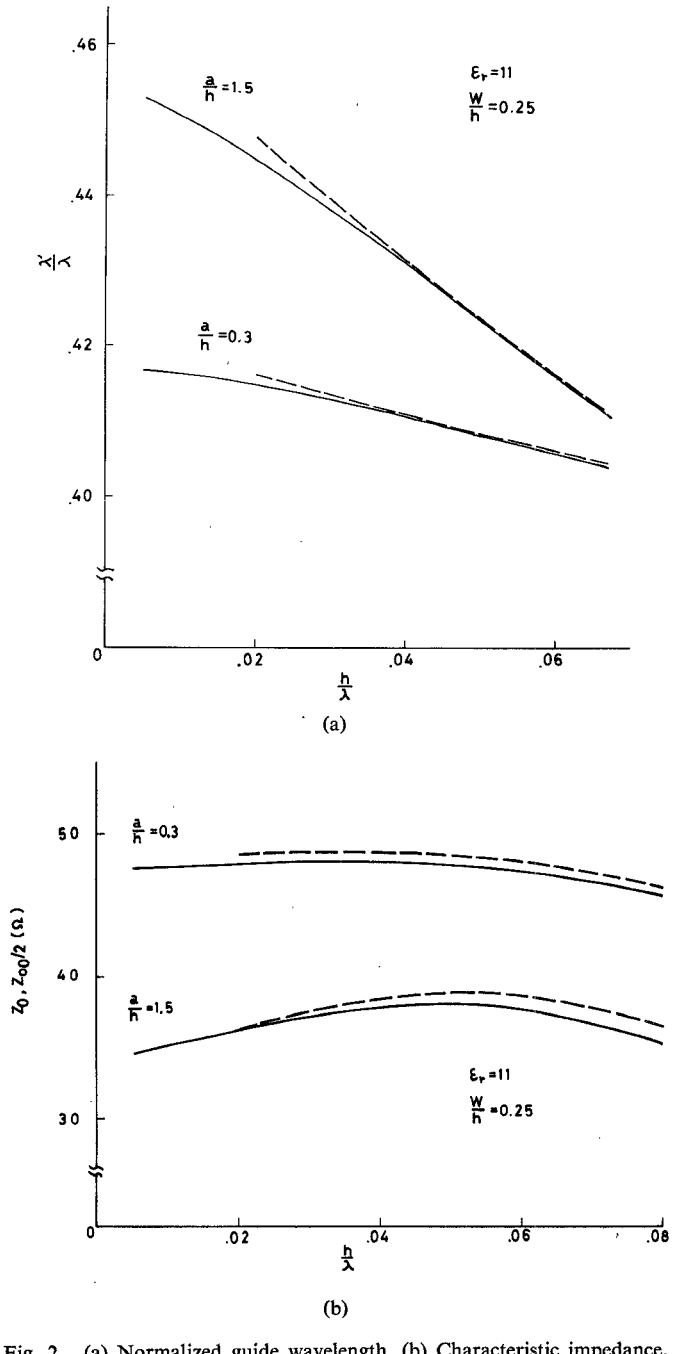

Fig. 2. (a) Normalized guide wavelength. (b) Characteristic impedance. $t/W = 0$; $W = b - a$. Solid line represents present method and broken line represents Knorr and Kuchlers' method [3].

defined in [3]. The difference is less than 1 percent for the dispersion characteristics [Fig. 2(a)] and less than 4 percent for the characteristic impedance [Fig. 2(b)]. It must be mentioned that the values of Knorr and Kuchler are available only for a graphical representation [3, fig. 6] and therefore may be somewhat in error.

Fig. 3 shows the effect of the metal-coating thickness on the guide wavelength and the characteristic impedance. When the t/W ratio is 0.02, the increase in the wavelength is about 1 percent and the decrease in the characteristic impedance is about 1.5 percent, and these are about the same as those of slot line [5].

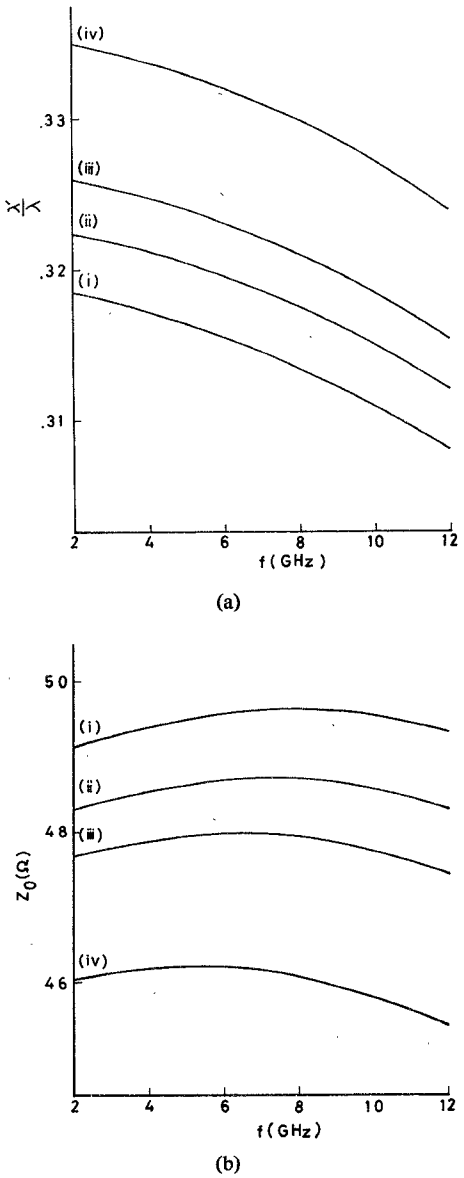

Fig. 3. (a) Normalized guide wavelength. (b) Characteristic impedance. $\varepsilon_r = 20$; $h = 1.0$ mm; $A = 0.2$ mm; $b = 0.7$ mm; $W = b - a$ (i) $t/W = 0.00$; (ii) $t/W = 0.02$; (iii) $t/W = 0.04$; (iv) $t/W = 0.10$.

These numerical calculation were carried out by the electronic computer FACOM 230-75. The calculation time was about 6 s for the wavelength and 0.5 s for the characteristic impedance.

References

[1] C. P. Wen, "Coplanar waveguide: A surface strip transmission line suitable for nonreciprocal gyromagnetic device applications," *IEEE Trans. Microwave Theory Tech.*, vol. MTT-17, pp. 1087–1090, Dec. 1969.
[2] M. E. Davis, E. W. Williams, and A. C. Celestini, "Finite-boundary corrections to the coplanar waveguide analysis," *IEEE Trans. Microwave Theory Tech.* (Short Papers), vol. MTT-21, pp. 594–596, Sept. 1973.
[3] J. B. Knorr and K. D. Kuchler, "Analysis of coupled slots and coplanar strips on dielectric substrate," *IEEE Trans. Microwave Theory Tech.*, vol. MTT-23, pp. 541–548, July 1975.
[4] T. Itoh and R. Mittra, "Dispersion characteristics of slot lines," *Electron. Lett.*, vol. 7, pp. 364–365, July 1971.
[5] T. Kitazawa, Y. Fujiki, Y. Hayashi, and M. Suzuki, "Slot line with thick metal coating," *IEEE Trans. Microwave Theory Tech.* (Short Papers), vol. MTT-21, pp. 580–582, Sept. 1973.
[6] T. Matsumoto and M. Suzuki, "Electromagnetic fields in waveguides containing anisotropic media with time-varying parameters," *J. Inst. Electron. Commun. Eng. Jap.*, vol. 45, pp. 1680–1688, Dec. 1962.

Analytical IC Metal-Line Capacitance Formulas

W. H. CHANG, MEMBER, IEEE

Abstract—**In semiconductor IC technology, capacitances formed by the multilevel interconnection metal lines usually dominate circuit performance. However, for lack of accurate formulas, a numerical method usually has to be used to determine these capacitances. Two analytical capacitance formulas were derived using approximate conformal mapping techniques. One formula gives the capacitance of a finite-thickness metal line over a conducting ground plane, or over a silicon surface. The other formula gives the capacitance of the same metal line, but with an additional conducting metal line over it. The formulas are most accurate for metal lines whose width exceeds the dielectric thickness; accuracy increases with linewidth. They are accurate to 1 percent for a metal line whose width is comparable to the dielectric thickness. With these simple formulas, statistical distribution of the metal-line capacitances can be easily determined in a few seconds of computer time.**

I. Introduction

In semiconductor integrated-circuit technology, capacitances formed by the metal interconnection lines usually dominate the circuit performance of the chip. It is therefore important for a circuit designer to determine metal-line capacitances accurately. Since the basic structure is similar to that of a microwave stripline, the structure has been well analyzed [1]–[8]. However, most of the treatment is either limited to a metal line of infinitesimal thickness, or a complicated numerical method is used to obtain the capacitances. The numerical method requires a computer and long computation time. Using conformal mapping techniques, accurate analytical capacitance formulas have been derived for a single rectangular metal line. Two analytical capacitance formulas are given: one gives the capacitance of a rectangular metal line over a conducting ground plane; the other gives the capacitance of the same metal line with two conducting ground planes, one above it and the other below it.

II. A Metal Line Over a Ground Plane

Fig. 1 shows a rectangular metal line above a ground plane. The metal has a width W, thickness t, and is separated from the ground plane by the distance h. The ground plane may be a silicon surface operating in an accumulation region. Because of the symmetry of the structure, only one-half of the structure needs to be considered. The half metal line $BCDE$ is extended to infinity at A and F in Fig. 2(a) to apply conformal mapping techniques and get a simpler formula. Boundary conditions are that the metal be at unity voltage, and ground plane be at 0 voltage, and the normal electric field vanishes along the lines MB and EKG. The Schwarz–Christoffel transformation (2)

$$\frac{\pi z}{h} = \frac{p+1}{p^{1/2}} \tanh^{-1} R + \left(\frac{p-1}{p^{1/2}}\right)\left(\frac{R}{1-R^2}\right) + \ln\left(\frac{Rp^{1/2}-1}{Rp^{1/2}+1}\right) \quad (1)$$

$$R = \left(\frac{w+1}{w+p}\right)^{1/2} \quad (2)$$

Manuscript received December 15, 1975; revised March 22, 1976.
The author is with the IBM System Products Division, East Fishkill, Hopewell Junction, NY 12533.